Memoirs of the Faculty of Science, Kyoto University, Series of Physics, Astrophysics, Geophysics and Chemistry, Vol. XXXIV, No. 2, Article 7, 1973.

SPIN CORRELATION PARAMETERS FOR 50 MeV PROTON-PROTON SCATTERING

BY

Takeo HASEGAWA

Department of Physics, Faculty of Science, Kyoto University, Kyoto

(Received May 12, 1972)

ABSTRACT

Two kinds of measurements of the spin correlation parameters at 90°$_{C.M.}$ for the 50 MeV proton-proton scattering have been performed. For the first step, the spin correlation parameters C_{KP} (90°$_{C.M.}$) and C_{NN} (90°$_{C.M.}$) at 52 MeV have been obtained by means of double scattering method, where the carbon polarimeter having nearly 40% analyzing power was used as a polarization analyzer. For the second step, the spin correlation parameters A_{xx} (90°$_{C.M.}$) and A_{yy} (90°$_{C.M.}$) at 47.5 MeV have been measured by using polarized beam and polarized target, where the nearly 50% polarized protons were provided by p-Ca elastic scattering and the meanly 35% polarized hydrogen target was constructed by means of dynamic polarization method. The incident proton spins were frequently flipped by a spin rotation solenoid and sometimes the target spins were inverted. Then, A_{xx} and A_{yy} were simultaneously measured by two pairs of detecting systems. The obtained results are as follows; C_{KP} (90°$_{C.M.}$; 52 MeV)$=0.13\pm0.11$, C_{NN} (90°$_{C.M.}$: 52 MeV)$=-0.034\pm0.095$, A_{xx} (90°$_{C.M.}$: 47.5 MeV)$=-0.713\pm0.032$ and A_{yy} (90°$_{C.M.}$: 47.5 MeV)$=-0.287\pm0.039$, and also A_{yy}/A_{xx} (90°$_{C.M.}$: 47.5 MeV)$=0.402\pm0.057$.
These results are compared with the phase shift analyses and the potential model in the medium energy region.

1. Introduction

To study the nucleon-nucleon interactions from the meson theoretical view point, especially to make clear the mechanism of the exchange of pions or bosons, the experimental investigations in the intermediate energy region (20~100 MeV) would be very advantageous, because in the higher energy region, many complicated phenomena will happen due to the effects of the inner structure of nucleon and hinder the simple phenomena to understand[1]. Therefore, very important informations would be obtainable from the proton-proton scattering at 50 MeV energy region, where such a dynamical effect as spin-orbit interaction plays an important role in addition to the static interactions of one pion exchange.

On the above basic standpoint, the Japanese experimental group for nuclear force study has proceeded the systematic measurements of the proton-proton scattering at 50 MeV by using the synchrocyclotron at *INS*, Tokyo. As one of the main projects on the above systematic investigations, we have measured the spin correlation parameters based on the two kinds of experimental methods in order to confirm the strength of the spin-orbit interaction in the intermediate energy region, and to make clear the origin of such dynamical effects.

The results have been already published in the short reports[2], and this paper is the experimental full report concerning to the measurements of the spin correlation parameters at 50 MeV.

2. Spin correlation parameters and nucleon-nucleon interaction in intermediate energy region

2-1. Scattering matrix and types of experiments

In the case of the nucleon-nucleon interaction, the scattering amplitude depends on the spin states of the two nucleons. Therefore, the scattering is described by a matrix in spin space[3] defined as

$$\begin{aligned} M=&a+b\,(\boldsymbol{\sigma}^{(1)}\cdot N-\boldsymbol{\sigma}^{(2)}\cdot N)+c\,(\boldsymbol{\sigma}^{(1)}\cdot N+\boldsymbol{\sigma}^{(2)}\cdot N)\\ &+m\,\boldsymbol{\sigma}^{(1)}\cdot N\,\boldsymbol{\sigma}^{(2)}\cdot N+g\,(\boldsymbol{\sigma}^{(1)}\cdot P\,\boldsymbol{\sigma}^{(2)}\cdot P+\boldsymbol{\sigma}^{(1)}\cdot K\,\boldsymbol{\sigma}^{(2)}K)\\ &+h\,(\boldsymbol{\sigma}^{(1)}\cdot P\,\boldsymbol{\sigma}^{(2)}\cdot P-\boldsymbol{\sigma}^{(1)}\cdot K\,\boldsymbol{\sigma}^{(2)}K) \end{aligned} \tag{1}$$

on the basis of the assumptions of space rotation invariance, space reflection invariance and time reversal invariance, where $\boldsymbol{\sigma}^{(1)}$ and $\boldsymbol{\sigma}^{(2)}$ are the Pauli spin matrices of the two nucleons and $\boldsymbol{P}$, $\boldsymbol{K}$ and N are the orthogonal unit vectors defined as

$$\left.\begin{aligned} &\boldsymbol{P}=\frac{\boldsymbol{k}_i+\boldsymbol{k}_f}{|\boldsymbol{k}_i+\boldsymbol{k}_f|}\ ,\\ &\boldsymbol{K}=\frac{\boldsymbol{k}_f-\boldsymbol{k}_i}{|\boldsymbol{k}_f-\boldsymbol{k}_i|}\\ \text{and}\quad &N=\frac{\boldsymbol{k}_i\times\boldsymbol{k}_f}{|\boldsymbol{k}_i\times\boldsymbol{k}_f|} \end{aligned}\right\} \tag{2}$$

here $\boldsymbol{k}_i$ and $\boldsymbol{k}_f$ are the incoming and outgoing momenta in the C. M. system.

The term b in Eq. (1) vanishes for the proton-proton scattering. Thus, we have to determine the complex coefficients a, c, m, g and h through the many types of experiments. Of course, all of the coefficients are not mutually independent because of the relationships based on the unitarity of the scattering matrix. Furthermore, these coefficients can be expressed in terms of the M matrix elements, which also can be represented in terms of phase shifts.

There are many possibilities of the experiments for the nucleon-nucleon scattering, since with the spin dependence the nucleons can be polarized in three directions, one along and two normal to the direction of motion as well as unpolarized. A basic form representing the relation between initial and final polarization states for the two nucleon scattering is given as[4]

$$I\langle S^{\mu}\rangle_f=\frac{1}{4}\sum_{\nu=1}^{16}\langle S^{\nu}\rangle_i\,Tr\,(MS^{\nu}\cdot M^{+}S^{\mu})\ , \tag{3}$$

where

$$I=\frac{Tr(M\rho_i M^{+})}{Tr\,\rho_i}=\frac{1}{4}\sum_{\nu=1}^{16}\langle S^{\mu}\rangle_i\,Tr(MS^{\nu}M^{+}) \tag{4}$$

is the differential cross section, ρ_i is the 4×4 spin density matrix for the initial system and $\langle S\rangle$'s are the expectation values of the spin operators S's. Hence, the spin state of the two nucleon system is specified by the expectation values of the 16 independent matrices

so that there are altogether $16^2(=256)$ different experiments possible corresponding to the initial and final spin states. These experiments are different experimentally, but some of them are identical to each other because of many theoretical relations; for example, half of the 256 observables vanish identically under the time reversal invariance, one case of which is the relation of the spin correlation parameters C_{NN} and A_{yy} in the present experiment, i.e. $C_{NN}=A_{yy}$ as described in later.

These observables can be expressed in terms of the coefficients a, c, m, g and h in the M matrix. Academically it is called complete experiment proposed firstly by Puzikov et al.[5] that at least five different experiments are needed in order to determine the M matrix or the complex coefficients a, c, m, g and h for the proton-proton scattering, where the measurements have to be carried out at all angles and in infinite accuracy, which are unpractical. Therefore, instead of determining the M matrix directly from the experimental data, usually the phase shift analyses are attempted to search the most probable set of phase shifts on the basis of some kinds of experimental data.

2-2. Spin correlation parameters

The spin correlation parameters are defined as the types of experiments that the final two Pauli spin matrices or the initial ones are concerned. The spin correlation parameters C_{KP}, etc. are the case of the former, in which an unpolarized beam is scattered from an unpolarized target and the polarizations of the scattered and recoiled nucleons $<\sigma_\alpha^{(1)}\cdot\sigma_\beta^{(2)}>_f$ are measured. On the otherhand, the A_{xx}, etc. are the case of the latter, in which the cross section is measured for the scattering of a polarized beam and a polarized target $<\sigma_\alpha^{(1)}\cdot\sigma_\beta^{(2)}>_i$ which are the time-reversed counterparts of the former. Some useful equations related to the experimental method are given as follows.

From Eqs. (3) and (4) for the simultaneous measurements on the polarizations of both scattered and recoiled nucleons for the scattering of unpolarized beam and unpolarized target, we have the spin correlation parameters $C_{\alpha\beta}$ defined as

$$I_0\, C_{\alpha\beta}\equiv I_0<\sigma_\alpha^{(1)}\,\sigma_\beta^{(2)}>_f=\frac{1}{4}\,Tr\,(MM^+\,\sigma_\alpha^{(1)}\,\sigma_\beta^{(2)})\ , \tag{5}$$

where α, $\beta=P$, K, N, as used in Eq. (3), and

$$I_0=\frac{1}{4}\,Tr\,(MM^+) \tag{6}$$

is the differential cross section in the common use; unpolarized beam and unpolarized target and no attention paid to final polarizations.

The nine measurements are possible conceptually. However, due to the form of the M matrix, only the four spin correlation parameters C_{NN}, C_{PP}, C_{KK} and $C_{KP}=C_{PK}$ are non-zero, which are illustrated schematically in Fig. 1.

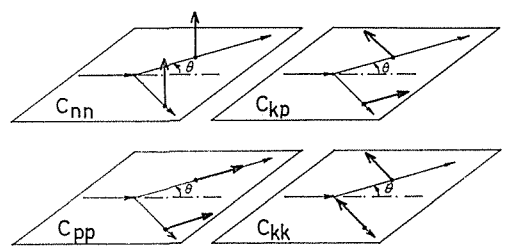

Fig. 1. Schematic representation of triple scattering spin correlation experiments.

The polarization analyzers for the scattered and recoiled nucleons are needed in the experiments, and moreover a spin rotator is necessary for the measurements of C_{PP} and C_{KK}.

On the otherhand, the differential cross section $I_{\alpha\beta}$ for the scattering of a polarized beam and a polarized target is given from Eqs. (3) and (4) as

$$I_{\alpha\beta}=\frac{1}{4}\,Tr(MM^{+})+\frac{1}{4}\,Tr\,(M\sigma_{\alpha}^{(1)}\,M^{+})\,\langle\sigma_{\alpha}^{(1)}\rangle_{i}$$
$$+\frac{1}{4}\,Tr\,(M\sigma_{\beta}^{(2)}\,M^{+})\langle\rho_{\beta}^{(2)}\rangle_{i}$$
$$+\frac{1}{4}\,Tr\,(M\sigma_{\alpha}^{(1)}\,\sigma_{\beta}^{(2)}\,M^{+})\,\langle\sigma_{\alpha}^{(1)}\rangle_{i}\,\langle\sigma_{\beta}^{(2)}\rangle_{i}\ . \tag{7}$$

Here, the first term is the same I_0 as Eq. (6), and the second and the third are the polarizations for the scattered and recoiled particles, respectively, that is

$$I_0\,P\equiv I_0\,\langle\sigma_n^{(1)}\rangle_f=\frac{1}{4}\,Tr\,(MM^{+}\,\sigma_n^{(1)})\ . \tag{8}$$

The tensor $A_{\alpha\beta}$ is defined as

$$I_0A_{\alpha\beta}=\frac{1}{4}\,Tr\,(M\sigma_{\alpha}^{(1)}\,\sigma_{\beta}^{(2)}M^{+})\,\langle\sigma_{\alpha}^{(1)}\rangle_{i}\,\langle\sigma_{\beta}^{(2)}\rangle_{i}\ , \tag{9}$$

which is also called the spin correlation parameter. Then, Eq. (7) is written as

$$I_{\alpha\beta}=I_0\,\{1+P(\delta_{\alpha n}\langle\sigma_{\alpha}^{(1)}\rangle_{i}+\delta_{\beta n}\langle\sigma_{\beta}^{(2)}\rangle_{i}$$
$$+A_{\alpha\beta}\langle\sigma_{\beta}^{(1)}\rangle_{i}\,\langle\sigma_{\beta}^{(2)}\rangle_{i}\}\ , \tag{10}$$

where $\delta_{\alpha n}$ and $\delta_{\beta n}$ are the Kronecker's delta. Here, the subscripts α and β are related to the unit vectors (x, y, z), where z is along the motion of the incident polarized nucleons, y is normal to the scattering plane and $x=y\times z$. The spin correlation parameters A_{xx}, etc. are shown in Fig. 2.

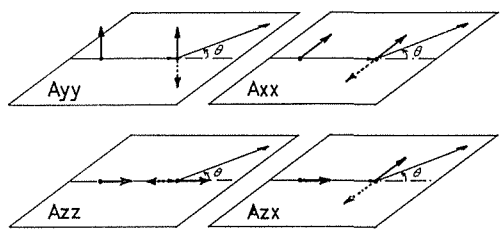

Fig. 2. Spin correlation parameters defined in the scattering of polarized beam by polarized target.

Experimentally, instead of the $I_{\alpha\beta}$, the so called asymmetry (e) of the spins parallel $(N^{\uparrow\uparrow})$ and antiparallel scattering $(N^{\uparrow\downarrow})$ may be measured, that is

$$A_{\alpha\beta}\,P_{\alpha}^{(1)}\,P_{\beta}^{(2)}\equiv e_{\alpha\beta}=\frac{N^{\uparrow\uparrow}-N^{\uparrow\downarrow}}{N^{\uparrow\uparrow}+N^{\uparrow\downarrow}} \tag{11}$$

for $90°_{c.m.}$ scattering ($P=0$ in Eq. (10)), where $P_{\alpha}^{(1)}$ and $P_{\beta}^{(2)}$ are the initial polarizations

of the beam and target, respectively.

There are the following relations between $C_{\alpha\beta}$ and $A_{\alpha\beta}$ under the time reversal invariance:

$$\left.\begin{aligned} A_{yy}&=C_{NN} \\ A_{zz}&=\sin\theta\, C_{KP}+\cos^2\frac{\theta}{2}\, C_{PP}+\sin^2\frac{\theta}{2}\, C_{KK}\ , \\ A_{xx}&=-\sin\theta\, C_{KP}+\sin^2\frac{\theta}{2}\, C_{PP}+\cos^2\frac{\theta}{2}\, C_{KK} \end{aligned}\right\} \tag{12}$$

and

$$A_{zx}=-\cos\theta\, C_{KP}+\frac{1}{2}\sin\theta\,(C_{PP}-C_{KK})\ ,$$

where θ is the observed angle in C.M. system.

The spin correlation parameters for the proton-proton scattering can be expressed in terms of the M matrix elements as

$$I_0(1-A_{yy})=I_0(1-C_{NN})=\frac{1}{2}\,|M_{SS}|^2\ , \tag{13}$$

$$I_0(1+A_{xx})=|M_{10}|^2\ , \tag{14}$$

$$I_0(A_{yy}-A_{xx})=|M_{01}|^2\ , \tag{15}$$

$$I_0C_{KP}=\frac{1}{2\sin\theta}\,(|M_{01}|^2-|M_{10}|^2) \tag{16}$$

and

$$I_0=\frac{1}{4}\,|M_{SS}|^2+\frac{1}{2}\,|M_{10}|^2+\frac{1}{2}\,|M_{01}|^2\ . \tag{17}$$

By using Eqs. (14), (15) and (16), we obtain the relations between C_{KP} and A_{xx} as

$$A_{xx}=\frac{1}{2}\,(C_{NN}-2\sin\theta\, C_{KP}-1)\ . \tag{18}$$

These matrix elements for 50 MeV proton-proton scattering can be expressed approximately in terms of phase shifts taken into account up to G-wave as follows;

$$\begin{aligned} |M_{SS}|^2\simeq&\frac{2}{k^2}\,\{1-\cos 2\delta(^1S_0)-5\delta(^1D^2)\sin 2\delta(^1S_0) \\ &+\frac{27}{4}\,\delta(^1G_4)\sin 2\delta(^1S_0)-\frac{e^2}{\hbar v}\sin 2\delta(^1S_0) \end{aligned} \tag{19}$$

$$\begin{aligned} |M_{10}|^2\simeq&\frac{2}{k^2}\left[\{\delta(^3P_0)-\delta(^3P_2)\}-\sqrt{6}\,\varepsilon_2-\frac{3}{2}\,\{\delta(^3F_2)-\delta(^3F_4)\}\right. \\ &\left.+\frac{3\sqrt{5}}{4}\,\varepsilon_4\right]^2 \end{aligned} \tag{20}$$

$$\begin{aligned} |M_{01}|^2\simeq&\frac{1}{2k^2}\left[3\{\delta(^3P_1)-\delta(^3P_2)\}+2\sqrt{6}\,\varepsilon_2-\frac{1}{4}\,\{7\delta(^3F_3)-15\delta(^3F_4)\}\right. \end{aligned}$$

$$+8\delta(^3F_2)\}-\frac{3\sqrt{5}}{2}\varepsilon_4\Big]^2 \tag{21}$$

where k is the wave number of the incident proton and v is the velocity of the incoming proton in Lab. system. As shown in Eqs. (14) and (15), $(1+A_{xx})$ and $(A_{yy}-A_{xx})$ are strongly sensitive to $\{\delta(^3P_0)-\delta(^3P_2)\}$ and $\{\delta(^3P_1)-\delta(^3P_2)\}$, respectively. Therefore, $A_{yy}(=C_{NN})$, A_{xx} and C_{KP} seem to be very effective observables to determine the p-wave splitting, which is very sensitive parameters to estimate the strength of the spin-orbit force as introduced by Gammel and Thaler[6].

2-3. Nucleon-nucleon interactions at 50 MeV energy region.

The Japanese theoretical study group for nuclear force has succeeded in understanding the mechanism of one pion exchange quantitatively in the outer region of nucleon ($r\gtrsim 1.5\mu^{-1}$: which is called the static region, where μ^{-1} is the pion Compton wave length[1),7]. For the next step on the basis of the meson theory, they have undertaken to investigate the nucleon-nucleon interactions in the inner region ($1.5\mu^{-1}\gtrsim r\gtrsim 0.7\mu^{-1}$) which is called the dynamical region[1], where such non-static effects as spin-orbit force would play an important role in addition to the static interactions of one pion exchange[7].

On the other hand, it was attempted to derive the phenomenological potentials from the 310 MeV proton-proton scattering data performed at Berkely[8]. Gammel and Thaler[6] have firstly proposed the one including a strong spin-orbit potential, and later by Hamada and Johnston[9] a more general potential including quadrutic spin-orbit term as well as spin-orbit term has been derived to represent the two-nucleon scattering data below 310 MeV, which is called the HJ-potential, and seems to be the most probable phenomenological potential at present. However, such a large spin-orbit interaction as the phenomenological potentials were not to be expected from the static potentials based upon the one and two pion exchange. Therefore, it was the main purpose for the Japanese school to make clear the origin of the spin-orbit force in the dynamical region from the meson theoretical view point[10].

In order to do so, it seemed to be more desirable to study the nucleon-nucleon interactions at medium energy region (20~100 MeV) than at such a higher energy region as 310 MeV, since as the energy is higher, such an innermost effect as a hard core structure contributes so complicatedly that the simple mechanism to be treated would be hindered. By considering the energy dependence of the differences in terms of phase shifts between the static potential based on one pion exchange and the non-static potentials with spin-orbit terms, the P-wave splitting at 50 MeV energy region would be very sensitive to the competition between the tensor type interaction and the spin-orbit type one[11]. In addition, from Eqs. (13) and (21) in the previous section, the spin correlation parameters at 50 MeV energy region are the effective observables to determine the p-wave splitting. The cross sections and the polarizations are not so sensitive to such non-static effects. At 50 MeV energy region $C_{KP}\gg 0$ is expected from the Gammel-Thaler potential where $|M_{01}|^2\gg M_{10}|^2\sim 0$, on the other, $C_{KP}\sim 0$ is expected from the static potential where $|M_{01}|^2\sim|M_{10}|^2$.[11] So, theoretically, the spin correlation parameters were considered to be very useful ones to estimate the strength of the spin-orbit force and to make clear the origin of such dynamical effects at medium energy region.

On the other hand, experimentally, by using the INS, Tokyo, synchrocyclotron, we could obtain the high intense 50 MeV proton beam which were distributed uniformly in time by means of the debunched extraction method[10]. Therefore, that machine was very suitable

for such a coincidence experiment as a spin correlation parameter measurement. Moreover, a carbon polarimeter was found to have a possible polarization analyzing power[12].

From the above considerations, for the first step, the measurements of the spin correlation parameters C_{KP} ($90°_{c.m.}$) and C_{NN} ($90°_{c.m.}$) at 50 MeV were performed by means of unpolarized beam and unpolarized target[2]. The phase shift analysis was attempted by Hoshizaki et al.[13] by using the C_{KP} and C_{NN} data as well as the differential cross sections which had been measured previously at INS[14]. According to the results[13], especially the $^3P_0$ phase shift at 50 MeV was somewhat higher than that expected from the Hamada-Johnston potential, which suggested that the spin-orbit force at 50 MeV would be not so strong as the one expected from the phenomenological potential like the Hamada-Johnston potential deduced from the higher energy experimental data.

In parallel to our experiments, the measurements of the polarization[15] and the different triple scattering parameters, i.e. the depolarization (D)[16], the A-parameter (A)[17] and the rotation parameter (R)[17] at 50 MeV have been performed at Rutherford Laboratory. There happened to be some different sets in the phase shift analyses according to which data were taken into account at 50 MeV[10),13], that is to say, when cross sections, P, C_{KP}, C_{NN} and D were used, the $\delta(^3P_0)$ were given at $14°\sim15°$, but when instead of the C_{KP}, C_{NN} and D, A and R were contained, then the $\delta(^3P_0)$ were set $11°\sim12°$, which was consistent with HJ-potential. These facts suggest that there are somewhat inconsistency existed among the experimental data and the proton-proton interactions at 50 MeV energy region have been not yet confirmed experimentally. According to the remeasurement of the differential cross sections by Sanada et al.[18] at 50 MeV, it has been obtained that the $\delta(^3P_0)$ is nearly the same as the HJ-potential[19]. More experimental studies were desirable at this energy region to remove the ambiguities discussed above and to construct the nucleon-nucleon interactions quantitatively.

It takes too long time to measure the C_{KP} and C_{NN} values in good statistics (a few percent) by means of unpolarized beam and unpolarized target and it will be difficult to remove the systematic errors completely in those measurements.

In the case of using polarized beam and polarized target, the spin correlation parameters $A_{\alpha\beta}$ can be obtained by only a single scattering process, and effective measurements are possible to overcome some difficulties in the unpolarized case. Then, without polarized ion sources, the polarized beam can be prepared by p-Ca elastic scattering at forward angles, which has been obtained at Rutherford Laboratory[20].

Therefore, for the second step, we have developed the polarized hydrogen target based on so-called dynamic polarization method, and performed the measurements of the spin correlation parameters A_{xx} and A_{yy} at $90°_{c.m.}$ for the 47.5 MeV proton-proton scattering by means of polarized beam and polarized target.

3. Measurement of C_{KP} and C_{NN} by means of unpolarized beam and unpolarized target.

3-1. Experimental method

As described in the previous section, the spin correlation parameter $C_{\alpha\beta}$ is obtained by the simultaneous measurement on the polarizations of the scattered and the recoiled nucleons produced by unpolarized beam and unpolarized target scattering.

For the first step, we have measured the spin correlation parameters C_{KP} and C_{NN} at $90°_{c.m.}$ for the 52 MeV proton-proton scattering by using the 53 MeV proton beam from the INS, Tokyo Synchrocyclotron. The experimental arrangement is shown in Fig. 3.

The 53 MeV unpolarized proton beam bombarded the 150 mg/cm thick polyethylene

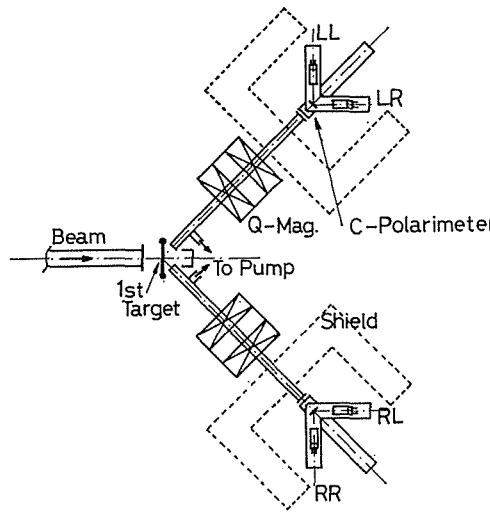

Fig. 3. Plan view of experimental arrangement for the C_{NN} measurement. For the C_{KP}, the polarimeters of both sides are positioned vertically.

target which had been moved automatically not to be melted away by the beam irradiation. The proton energy at the center of the polyethylene target was estimated 52.3 MeV by considering the energy loss. In order to reject the background counts as many as possible, both scattered and recoiled protons to $44.6° \pm 2°$ Lab. in horizontal plane were focussed onto the polarization analyzers by the quadrupole magnets, which currents were adjusted in such a way that only the required protons were effectively focussed and the minimum focussing images were obtained.

The proton-carbon elastic scattering at $40°_{Lab}$ was chosen as the polarization analyzer

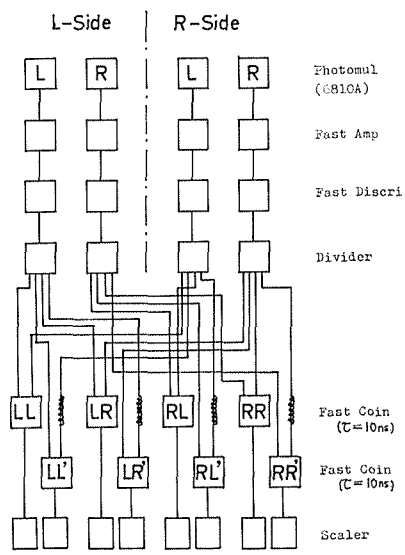

Fig. 4. Electronic block-diagram for the C_{KP} or C_{NN} measurement.

which analyzing power was estimated 0.39 ± 0.03 from the previous measurement[12] of the polarization of p-C scattering under the same geometrical conditions, that is, the 270 mg/cm^2 thick graphite plates as the second targets and the solid angles of 0.15 steradians were used. Four plastic scintilation counters with 6810A photomultipliers were placed on the rotating stands which were adjusted in vertical plane or horizontal one corresponding to the C_{KP} or C_{NN} measurement, respectively. The protons doubly scattered simultaneously from both left and right polarimeters were detected in coincidence within $2\tau=20$ nsec resolving time. The electronic brockdiagram is shown in Fig. 4.

Such four kinds of coincidence counts as UU, DD, UD and DU for the C_{KP} measurement and LL, RR, LR and RL for the C_{NN} one were measured together with the 100 nsec delayed coincidence counts from which the random coincidence counts were estimated, where UU is the number of coincidence counts between the upside detector of the lefthand polarimeter and the upside one of the righthand polarimeter, etc.. Then, the so-called asymmetries wer obtained by taking the geometric means as

$$C_{KP}P_L\cdot P_R\equiv e_{KP}=\frac{\sqrt{UU\cdot DD}-\sqrt{UD\cdot DU}}{\sqrt{UU\cdot DD}+\sqrt{UD\cdot DU}} \tag{22}$$

and

$$C_{NN}P_L\cdot P_R\equiv e_{NN}=\frac{\sqrt{LL\cdot RR}-\sqrt{LR\cdot RL}}{\sqrt{LL\cdot RR}+\sqrt{LR\cdot RL}} \tag{23}$$

Here, P_L and P_R are the analyzing powers of the carbon polarimeters of both sides. The detector positions were exchanged by rotating the analyzers along the axes as frequently as possible in order to eliminate the geometrical asymmetries of the detecting systems.

3-2. Experimental results

The measurements of C_{KP} and C_{NN} have been performed in two steps at an interval of one year, i.e. in the first, only the C_{KP} has been measured, and in the second, both the C_{NN} and C_{KP} have been done. The latter results for the C_{KP} was consistent with the former one within the statistical errors, so the final C_{KP} value was deduced by taking the weighted mean between the two measurements.

By using the Eqs. (22) and (23), the final results of the C_{KP} and C_{NN} at 52 MeV are obtained as follows,

$$C_{KP}(90^\circ_{c.m.},\ 52\ \text{MeV})=0.13\pm0.11$$

and

$$C_{NN}(90^\circ_{c.m.},\ 52\ \text{MeV})=-0.034\pm0.095,$$

where the indicated errors are the statistical ones only and $(P_L\cdot P_R)=(0.39)^2=0.152$ are used.

In order to estimate the systematic errors which were caused by the misalignment of the apparatus and the finite geometrical effects in the experimental conditions, the individual asymmetries for the four cases corresponding to the four counters (I, II, III, IV) being (LU, LD, RU, RD), (LU, LD, RD, RU), (LD, LU, RD, RU) and (LD, LU, RU, RD) for the C_{KP}, (LL, LR, RL, RR), (LL, LR, RR, RL), (LR, LL, RR, RL) and (LR, LL, RL, RR) for the C_{NN}, were compared each other. Then, the all asymmetries agreed within the statistical errors, which meant that the systematic errors were considered to be less than the statistical one. Of course, if they were, the main part of them were expected to be eliminated by exchanging

the detector positions as described above by rotating the polarimeters.

For comparison with A_{xx} experiment, the obtained C_{KP} value which is the only one measurement in this energy region is transformed to the A_{xx} by using the relations of Eq. (18) as well as the C_{NN} value, that is, at $90°_{c.M.}$, $A_{xx}=\frac{1}{2}(C_{NN}-2C_{KP}-1)=-0.647\pm0.120$ is obtained.

4. Measurement of A_{xx} and A_{yy} by means of polarized beam and polarized target.

4-1. General description

For the scattering of polarized beam and polarized target, the spin correlation parameter $A_{\alpha\beta}$ is determined by measuring the asymmetry of the scattering yields corresponding to the incident and target proton spins being parallel and antiparallel. This measurement based on a single scattering is undoubtedly more advantageous than that based on double scattering process in order to make the statistical errors smaller and smaller effectively and to reduce the existing systematical errors as far as possible. For the second step, we have developed the polarized proton target and measured simultaneously the spin correlation parameters A_{xx} and A_{yy} at $90°_{c.M.}$ for the 47.5 MeV proton-proton scattering by means of polarized beam and polarized target. The experimental arrangement is shown schematically in Fig. 5.

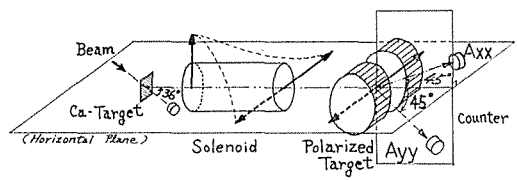

Fig. 5. Schematical representation of experimental method for the simultaneous measurement of the spin correlation parameters A_{xx} and A_{yy}.

The polarized protons were prepared by the p-^{40}Ca elastic scattering. The elastically scattered protons which were polarized normal to the scattering plane were passed through a solenoid coil which had rotated the spins $\pm90°$ and led to the polarized target after being focussed by a quadrupole magnetic lense system. The polarized hydrogen target was constructed by means of dynamical method. As the target was polarized horizontally, the incident spins and the target ones were parallel or antiparallel in the horizontal plane. Then, the spin correlation parameters A_{xx} and A_{yy} were obtained by measuring the scattering asymmetries at $45°_{Lab}$ in the horizontal plane and in the vertical one, respectively.

To perform the experiment, both incident beam polarization and target one had to be determined precisely. However, it was difficult to measure the target polarization precisely in our method discussed later, so we have obtained the spin correlation parameters by normalizing to the ones at 26.5 MeV measured by Saclay Group[21], that is, the measurement of the asymmetries at 26.5 MeV as well as at 47.5 MeV have been alternatively made, and by comparing them with the Saclay data, the product (P_1. P_2) of the beam polarization (P_1) and the target one (P_2) was determined. Thus, A_{xx} and A_{yy} were obtained by the relations as follows,

$$(P\cdot P)=\frac{e_{xx(yy)}\ (26.5\ \text{MeV: Present})}{A_{xx(yy)}(26.5\ \text{MeV: Saclay})} \tag{24}$$

and

$$A_{xx(yy)}(47.5\ \text{MeV})=\frac{e_{xx(yy)}\ (47.5\ \text{MeV})}{(P_1\cdot P_2)}=\frac{e_{xx(yy)}\ (47.5\ \text{MeV})}{e_{xx(yy)}\ (26.5\ \text{MeV})}\cdot A_{xx(yy)}\ (26.5\ \text{MeV: Saclay}) \tag{25}$$

where e is the asymmetry of the spin parallel scattering ($N^{\uparrow\uparrow}$) and the antiparallel one ($N^{\uparrow\downarrow}$), that is

$$e=\frac{N^{\uparrow\uparrow}-N^{\uparrow\downarrow}}{N^{\uparrow\uparrow}+N^{\uparrow\downarrow}}$$

The detailed descriptions concerned to the polarized beam, the polarized target and the detecting systems are given in the following sections.

4-2. Polarized beam

The 53.7 MeV proton beam extracted from the 180 cm synchrocyclotron at INS, Tokyo, bombarded the 3 mm thick *Ca*-target which was made by rolling the natural calcium metal and kept airtight by 1 μm nickel foil. The protons elastically scattered to $\theta_{Lab.}=36.5°\pm1.5°$ were polarized 50% normal to the scattering plane, which was checked by double scattering method under the same geometrical conditions.

The scattered protons were passed through the 160 cm length solenoid coil to rotate the spins to $\pm90°$ in the plane normal to the moving direction. After passing through the solenoid, the protons were focussed onto the polarized target by two pairs of quadrupole magnets. In order to obtain the optimum image and not to be shifted its position by changing the current and the polarity of the solenoid and the quadrupole magnets, the setting of them and the adjusting the current were performed by looking the image and the energy spectra at target position by using *X*-ray films and a scintilation counter, respectively.

The plan view of experimental arrangement is shown in Fig. 6.

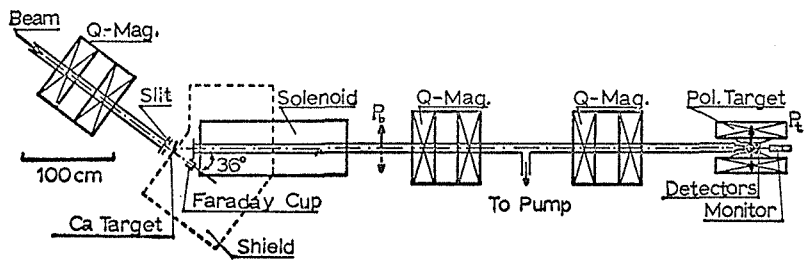

Fig. 6. Plan view of experimental arrangement for the A_{xx} and A_{yy} measurement.

The proton energy at the polarized target center was estimated 47.5 MeV$\pm$2.3 MeV by considering the kinemtics and the energy loss in the Ca target and the polarized target system.

4-3. Polarized proton target

The polarized proton target used in the present experiment was constructed by means

of dynamic polarization method developed firstly by Abragam et al. and Jeffries et al. independently.[22] The protons in the so-called LMN crystal (La_2 ($1\%Nd^{3+}$) $Mg_3(NO_3)_{12}$. 24 H_2O) were polarized through the magnetic dipole interaction between protons and electrons existed excessively in the paramagnetic ions by saturating the partially forbidden trasitions of electron spin resonance under the strong magnetic field and in the low temperature. Fig. 7 shows the energy levels of an electron spin loosely coupled to a nucleus of spin 1/2 in the two kinds of magnetic field. The population distributions are also shown on the right side of the figure, where the population (A) is in the case of the thermal equilibrium.

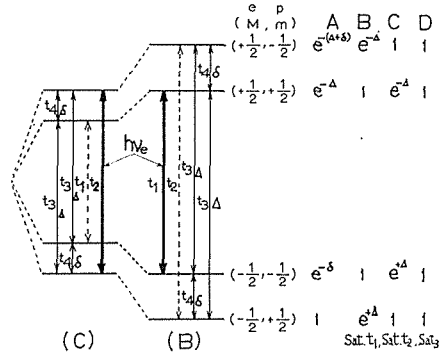

Fig. 7. Separated energy levels of the dipole interaction between electron spins and proton ones in two kinds of magnetic fields. t_1 and t_2 are forbidden transition, and t_3 and t_4 are allowed one. Populations in four cases are also shown in kT unit.

Now, saturation of the forbidden transition t_1 by the micro wave power supply leads to the population (B) which corresponds to the positive polarization. The polarization may be reversed by changing the magnetic field slightly and saturating the another forbidden transition t_2, that is the case (C). Thus, polarized target system consists of a strong magnetic field, an electron spin resonance system with micro wave power supply, a nuclear magnetic resonance system detecting the target polarization, a cooling system to cool down the LMN crystal, and a target part allowing the proton transit.

The 18,600 Oe magnetic field was prepared by the magnet with the pole area 14 cm in diameter and the 5 cm pole gap and guranteed the field stability of 2×10^{-5} and the field homogeneity of 3×10^{-5} at the target area.

The 70 GH_z micro wave power was used corresponding to the magnetic field. About the 100 mW power was generated by the Varian VC104K klystron and sent to the cavity through the Cu-Ni wave guide and the tapered guide. The LMN crystal was mounted in the ditch inside the cavity by the paste Kel-F with no hydrogen.

The vertical type cryostat as shown in Fig. 8 with a liquid helium container and a cooling room was constructed. The detailes of the cryostat are described in another publication[23]. As shown in Fig. 8, the cooling room were inclined about 15° from the vertical by considering the 50 MeV proton beam trajectory in the magnetic field.

The flow of liquid helium from the container was controlled by two needle values before and after passing through the heat exchanger and was spouted upon the LMN crystal from the hole on the inner wall of the cavity. The evapolated helium gas in the cavity was pumped out through the 5 μm cupper foil having many holes of 0.5 mm in diameter to the recovering

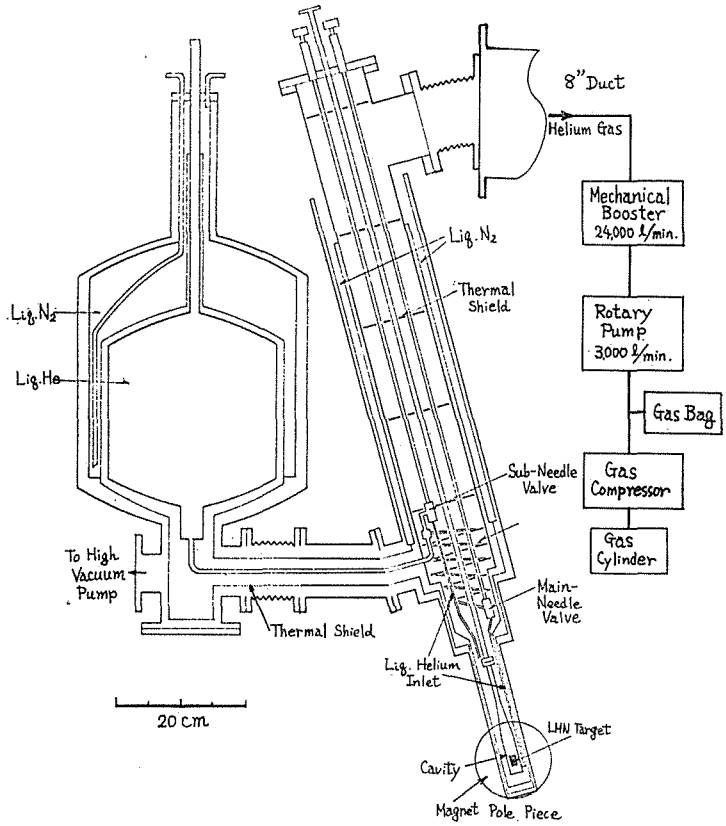

Fig. 8. Vertical type cryostat for polarized proton target used in present experiment.

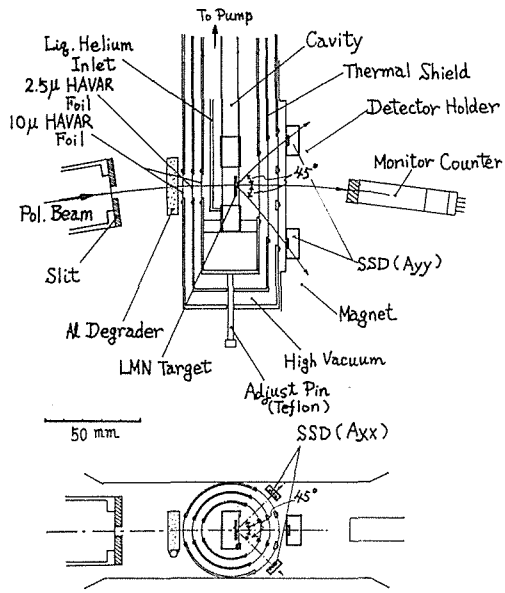

Fig. 9. Horizontal and vertical cross sections of polarized target and detecting system in the magnet.

system by a 24000 1/min. mechanical booster pump and a 3000 1/min. rotary pump through an 8″ vacuum duct. In such a way the temperature at the vicinity of the LMN crystal has reached to 1.2°K with 100 mW micro wave power supply.

Fig. 9 shows the details of the target part. The 1 mm thick and 10×10 mm^2 LMN crystal was used.

The magnet was placed so that the bended beam might be passed through it's center. The beam path in the magnetic field was ascertained by using the X-ray films which were put at some positions in the pole gap. The cryostat was set carefully at the center of the pole gap by means of the adjustable stand. The position-adjustable pin made from teflon was installed at the tip of the cryostat in order to connect the contraction due to cooling.

The target polarization was estimated by detecting the enhanced NMR signals, which were compared with the ones at thermal equilibrium. The static polarization P_0 at thermal equilibrium under the temperature (T) and the magnetic field (H) is expressed as

$$P_0 \simeq \frac{g_N \beta H}{2kT} \simeq 10^{-7} \frac{H}{T} , \tag{26}$$

and the enhanced polarization P is expressed as

$$P = \varepsilon P_0 , \tag{27}$$

where ε is called the enhancement factor, and g_N and β represent the g-factor of proton and Bohr magneton, respectively.

However, the NMR signals at thermal equilibrium was very small and the signal to noise ratio was poor, so it was difficult to detect the target polarization precisely from the NMR signals only. Therefore, in the present experiment the product (P_1P_2) of the beam polarization (P_1) and the target one (P_2) was obtained by measuring the asymmetries at 26.5 MeV and by comparing them with the A_{xx} ($90°_{c.m.}$) and A_{yy} ($90°_{c.m.}$) values which had been measured precisely by Saclay group in 1967[21]. A 6 mm thick Al-plate was used as an energy degrader, which was set in front of the cryostat. The shift of the proton path in the magnetic field at 26.5 MeV from the case at 47.5 MeV was about 1 mm, which was regarded to be negligible small by considering the dimensition of the beam spot and the solid angles of detecting system.

Thus, the measurements of the asymmetries for spin parallel and antiparallel were performed alternately at 47.5 and 26.5 MeV by flipping the beam spin frequently by spin rotating solenoid, and also sometimes by inverting the target spin by changing the magnetic field slightly in order to cancel the geometrical asymmetries.

4-4. Detecting system

To measure the A_{xx} ($90°_{c.m.}$) and A_{yy} ($90°_{c.m.}$) simultaneously, the two pairs of detectors were placed in horizontal and vertical scattering planes, respectively. Each pair consisted of the two rectangular type solid state detectors which had 2.5 mm thick and 2×4 mm^2 detecting area and was mounted on the holder inside the pole pieces of the magnet. These detectors were set at proper positions corresponding to 44.6° scattering in Lab. system by considering the bending of the protons in magnetic field. The scattered and recoiled protons were detected in coincidence by them to reject the protons scattered from other elements contained in the LMN crystal and the coincident energy spectra were recorded in the 256 ch. pulse heigh analyzer. The block diagram of the detecting systems are shown in Fig. 10.

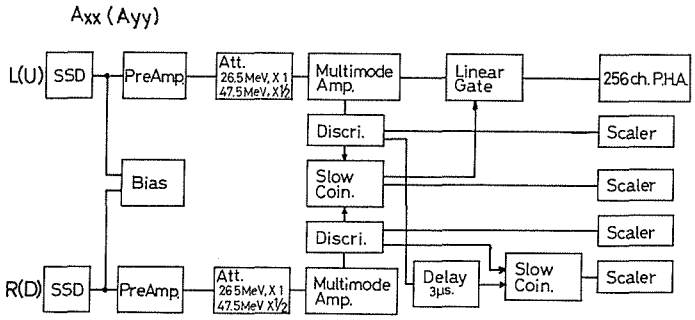

Fig. 10. Block-diagram of counting system for the A_{xx} and A_{yy}.

The Faraday cup at the rear of the Ca target and the plastic scintilation counter at the back of the polarized target were used as the monitors.

4-5 Experimental results

The measurement was performed by using the primary proton beam of 53.75 MeV which corresponded to E_p=47.5 MeV at the polarized target by considering the energy losses.

In order to minimize the errors caused from the fluctuation of the target polarization from time to time, the incident proton spins were flipped every about ten minutes by the spin-rotating solenoid, and the measurements at 47.5 MeV and 26.5 MeV were repeated alternately. Moreover, the target spin was flipped every about ten hours by changing the magnetic field slightly so as to eliminate the small shift of the beam path due to the solenoid field and the geometrical asymmetries of the detecting system. The NMR signals were recorded continuously to monitor the target polarization.

At the beginning of the experiment, liquid helium happened to stay in the target room because of the needle value being out of order. Then, for the 26.5 MeV measurement, the scattered protons could not come out from the cryostat by losing full energy in the liquid helium, although little affected for the 47.5 MeV. So, the target polarization in that case was estimated only from the NMR signals which were compared with the one in the normal conditions being no liquid helium to soak the target crystal.

The four kinds of counts as $N^{\uparrow\uparrow}$, $N^{\uparrow\downarrow}$, $N^{\downarrow\uparrow}$ and $N^{\downarrow\downarrow}$ corresponding to the spin directions of the incident and target protons were obtained by the vertical (A_{xx}) and horizontal (A_{yy}) detecting systems at 26.5 and 47.5 MeV. In order to eliminate the spurious asymmetries, the so-called asymmetries were calculated by using the geometric means of above counts, that is

$$e=\frac{\sqrt{N^{\uparrow\uparrow}\cdot N^{\downarrow\downarrow}}-\sqrt{N^{\uparrow\downarrow}\cdot N^{\downarrow\uparrow}}}{\sqrt{N^{\uparrow\uparrow}\cdot N^{\downarrow\downarrow}}+\sqrt{N^{\uparrow\downarrow}\cdot N^{\downarrow\uparrow}}}\ . \tag{28}$$

(i) At 26.5 MeV, we obtained the asymmetries
$e_{xx}=-0.153\pm0.019$ and $e_{yy}=-0.132\pm0.026$.

By using the Saclay result[21] that $A_{xx}=-0.926$ and $A_{yy}=-0.732$ at 26.5 MeV which were deduced by assuming A_{xx} $(90°_{c.M.})=-0.984$ at 11 MeV, we obtain the product of the beam polarization (P_1) and the target one (P_2) as
$(P_1P_2)_{xx}=0.166\pm0.021$ and $(P_1P_2)_{yy}=0.180\pm0.035$,

from which by taking the weighted mean we obtained

$(P_1P_2)=0.169\pm0.018$.

(ii) At 47.5 MeV, we obtained the asymmetries,

$e_{xx}=-0.121\pm0.005$

and

$e_{yy}=-0.049\pm0.007$.

By using the (P_1P_2) estimated from the 26.5 MeV measurement, we obtained the final results

A_{xx} ($90°_{c.m.}$ 47.5 MeV)$=-0.713\pm0.032$

and

A_{yy} ($90°_{c.m.}$ 47.5 MeV)$=-0.287\pm0.039$,

where the indicated errors are statistical only. The normalization error which effected in comparing process with the Saclay data at 26.5 MeV was supposed to be about 10% by considering the statistical errors at 26.5 MeV and the ambiguities of the NMR signals which were used to estimate the target polarizations in the case of no 26.5 MeV measurement discussed above and also the small differences of the proton paths at 47.5 and 26.5 MeV in magnetic field.

As the measurements were performed simultaneously for the A_{xx} and A_{yy} and alternately at 26.5 and 47.5 MeV, the following ratios are obtainable independently of both of the beam polarization and the target one and also the Saclay data, that is

$$(A_{yy}/A_{xx})_{47.5\ \mathrm{MeV}}=(e_{yy}/e_{xx})_{47.5\ \mathrm{MeV}}=0.402\pm0.057\ ,$$

$$(A_{yy}/A_{xx})_{26.5\ \mathrm{MeV}}=(e_{yy}/e_{xx})_{26.5\ \mathrm{MeV}}=0.863\pm0.200\ ,$$

$$A_{xx}(47.5\ \mathrm{MeV})/A_{xx}(26.5\ \mathrm{MeV})=e_{xx}(47.5\ \mathrm{MeV})/e_{xx}(26.5\ \mathrm{MeV})$$
$$=0.791\pm0.104$$

and

$$A_{yy}(47.5\ \mathrm{MeV})/A_{yy}(26.5\ \mathrm{MeV})=e_{yy}(47.5\ \mathrm{MeV})/e_{yy}(26.5\ \mathrm{MeV})$$
$$=0.371\pm0.090.$$

These are very useful values in comparing with other experimental results.

As there might be some possibilities of the background counts due to such quasi-free scatterings as (p, 2p) reactions in the *LMN* crystals, we have measured the angular correlations in such a way that the one detector was fixed at 44.6° and the other was changed from 30° to 60° in Lab. system. As the result, the protons from the (p, 2p) reactions were found to be negligible compared with the *p-p* scattering, which was consistent with the very small (*p*, 2*p*) reaction cross sections in this energy region.

The random coincident counts were maximum 10% of the true one, which were perhaps neutrons mainly. However, the obtained asymmetries were almost all independent how to subtract the background counts in the measured spectra.

The non-uniformity of the polarizations might be happened by the non-uniform distributions of the micro wave field and the temperature in the target crystal. In our case, the untuned oversize cavity and the effective cooling system were used, so the uniform distribution of the target polarization was to be expected.

It is known that the irradiation of the intermediate energy protons on the *LMN* crystals reduces the target polarization by one half for $(3\sim5)\times10^{13}$ protons/cm^2 [24]. In the present case the total irradiation was about 10^{11} protons, and little depolarization due to radiation damage was found. By using the (P_1P_2) value and the beam polarization $P_1=0.50$, we found the mean target polarization $P_2=0.34$, which was consistent with the one estimated

from the *NMR* signals only.

6. Discussion

The present results are shown in Fig. 11 with other experimental data[21),25)~27)] and some predicted values based upon the phase shift analyses[28)] and the potential model[29)] in the intermediate energy region. In Fig. 11, the C_{KP} being transformed to the A_{xx} by using Eq. (18) is also shown.

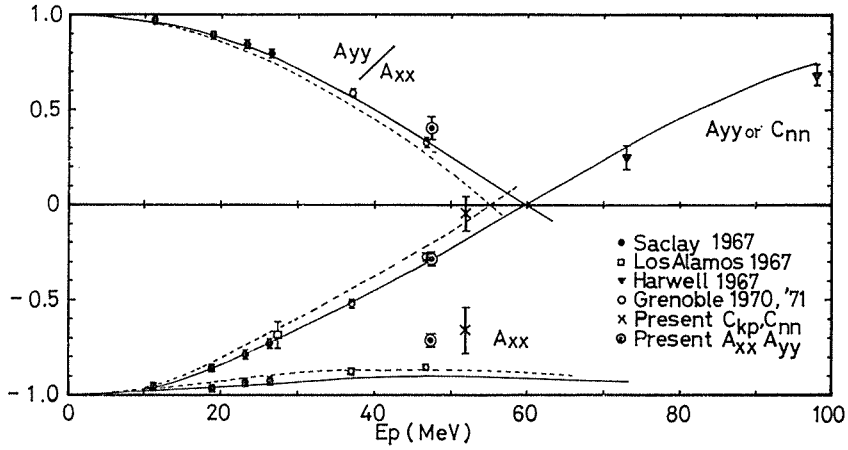

Fig. 11. Present and other experimental results in the intermediate energy region. For the references, see refs[21),25)~27)]. The solid lines and the dashed ones are the predicted values based on Livermore phase shift analysis[28)] and the Tamagaki potential (HC–81)[29)]. The C_{KP} is shown as transformed to A_{xx} by using the relation.

For the two kinds of experimental methods in our measurements, the A_{xx} and A_{yy} results at 47.5 MeV are fairly consistent with the C_{KP} and C_{NN} ones at 52 MeV by considering their small energy dependencies.

Recently, the A_{xx} and A_{yy} measurements at 46.9 MeV[29)] and 37.5 MeV[26)] have been performed at Grenoble by using polarized ion source and polarized target. According to their results at 46.9 MeV, $A_{xx}=-0.850\pm0.015$ and $A_{yy}=-0.275\pm0.010$ are obtained, which are apparently inconsistent with ours, that is to say, there is a large discrepancy for the A_{xx} values, although the A_{yy} values are in fairly good agreement. As the ratio A_{yy}/A_{xx} in our measurement at 26.5 MeV agrees well in statistics with 0.788 ± 0.007 obtained at Grenoble, the above discrepancy seemed not to be caused by the normalizing process.

Several possibilities were examined as the causes producing above inconsistency in the A_{xx} and A_{yy} results, that is, (i) the respective scattering centers in the target crystal to the A_{xx} and A_{yy} detecting systems might not be the same and also the polarizations at each center were different, (ii) the scattering angle for the A_{xx} might not be $90°_{C.M.}$ and (iii) the estimation of the scattering energy might be incorrect. As described in the previous section, we used the untuned oversized cavity and the effective cooling system, so the uniform polarization distribution was to be maintained not like the case (i). Also, the discrepancy being too large to be caused by the misalignment of the detecting system and the mistakes of the energy estimation, it was difficult to consider the errors resulted in the case (ii) and (iii). For

other careful considerations on the possible error sources included in our measurements, we could not find any systematic errors to interprete such a discrepancy for the A_{xx}.

As described shortly in § 2–4, the phase shift analysis was attempted by Hoshizaki et al. by using the C_{KP} and C_{NN} values at 50 MeV, and resulted in the important informations that the $\delta(^3P_0)$ was about 14∼17/ and the spin-orbit force at 50 MeV might not be necessarily so strong as at higher energy region. However, in order to complete the phase shift analysis and to confirm the character of the spin orbit interaction in this energy region, the C_{KP} and C_{NN} experiment was not sufficient in statistics and in consistency with other triple scattering parameters obtained at Rutherford Laboratory.

The above preliminary informations obtained from the C_{KP} and C_{NN} measurements has been confirmed by the A_{xx} and A_{yy} results. The solid curves in Fig. 11 represent the values predicted from the recent energy dependent phase shift analysis developed at Livermore (referred to as *XEDA*)[28] which is consistent with the Hamada-Johnston potential. The predicted A_{yy} agrees quite well with the present C_{NN} and A_{yy}, whereas the A_{xx} shows large discrepancy of 6 standard deviations with the present experiments, and also shows discrepancy 3.7 deviations with the Grenoble result. For the predicted values from the phase shift analysis at 50 MeV by Hoshizaki[19] including the cross section data remeasured by Sanada et al., nearly the same considerations are given.

For the A_{yy}/A_{xx} values, which are useful for comparison because of being independent with beam and target polarization, one can see the systematic behavior showing the significant discrepancy between the experimental data and the predicted values for 10 to 50 MeV energy region, which indicates that the *XEDA* phase shift analysis is not yet complete. By considering the experimental A_{yy} values being fairly consistent with the predicted ones, this incompleteness should be resulted in the ambiguity of $^3P_0$-wave phase shift.

The dotted lines in Fig. 11 are the values predicted from the Tamagaki potential (*HC*–81)[29] which is based upon the meson theoretical treatment. The better fit than the *XEDA* has been obtained for the 30 to 50 MeV A_{xx} values, but not for the A_{yy}. Also, the *HC*–81 potential seems not to be able to explain the energy dependecy of the spin correlation parameters.

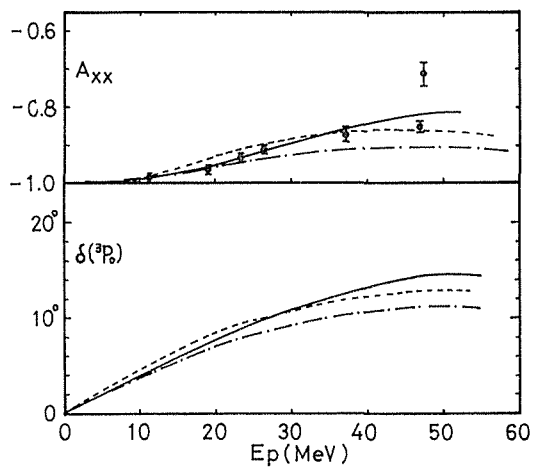

Fig. 12. Estimation of the $^3P_0$ wave phase shift fitting to the experimental A_{xx} data. The solid lines are the curves smoothly connecting the experimental points. The dashed and the dashed dotted lines are the predictions based on the Tamagaki potential[29] and the recent Livermore phase shift analysis[28].

In orther to examine the energy dependence of $\delta(^3P_0)$, we have tried to reconstruct the A_{xx} data by changing only the $\delta(^3P_0)$ from the *XRDA* in this energy region, where the weighted mean of the A_{xx} values between the present and the Grenoble data is used for 47.5 MeV. The estimated $\delta(^3P_0)$ is shown by solid line in Fig. 12, in which the recontructed A_{xx} values and the predicted values from the *XEDA* and the *HC*–81 are also shown for comparison.

Apparently from Fig. 12, the deduced $\delta(^3P_0)$ at 50 MeV is about three degrees larger than that of the *XEDA*, which suggests that the spin-orbit force in this energy region is not so strong as one at higher energy region. The *HC*–81 potential is not able to reproduce the energy dependency of the deduced $\delta(^3P_0)$. In order to explain such energy dependency based on the Tamagaki potential, the energy dependency of the pion-nucleon coupling constant might be taken into account[30]. Of course, more accurate considerations should be based upon the detailed phase shift analysis, which will be shown in another publication in near future.

Since there remain some ambiguities due to the discrepancy of the A_{xx} between the present and the Grenoble data, more extensive measurements in the intermediate energy region especially in 50 to 100 MeV region are desired in order to confirm the phase shifts and make clear the mechanism of the proton-proton scattering.

ACKNOWLEDGEMENTS

We would like to express our sincere gratitude to Prof. K. Nisimura for his helpful encouragement and valuable discussions. We are pleased to give thanks to the other coworkers, Profs. J. Sanada, S. Kobayashi, N. Ryu, K. Fukunaga, H. Hasai, D. C. Worth, H. Imada and Y. Hiratate for the C_{KP} and C_{NN} measurements, and Drs. N. Horikawa, T. Nakanishi, M. Saito, T. Saito, S. Sugimoto, E. Takasaki, H. Yeno and T. Yamaki for the A_{xx} and A_{yy} measurement, for their help in performance of this experiment and for useful discussions.

REFERENCES

1) M. Taketani et al.: Prog. Theor. Phys. **6** (1951) 581 See also, Prog. Theor. Phys. Suppl. **3** (1961)
2) C_{KP} and C_{NN}: K. Nisimura et al.: Prog. Theor. Phys. **29** (1963) 616; Prog. Theor. Phys. **30** (1963) 719 A_{xx} and A_{yy}: K. Nisimura et al.: Phys. Letters **30B** (1969) 612. See also, Ref. 10)
3) L. Wolfenstein and J. Ashkin: Phys. Rev. **85** (1952) 947.
4) See, for example, N. Hoshizaki: Prog. Theor. Phys. Suppl. **42** (1968) 107; See also, J. Raynal: Nucl. Phys. **28** (1961) 220.
5) L. Puzikov et al.: Nucl. Phys. **3** (1957) 436.
6) J. L. Bammel and R. M. Thaler: Phys. Rev. **107** (1957) 291.
7) M. Taketani et al.: Prog. Theor. Phys. Suppl. **39** (1967).
8) O. Chamberlain et al.: Phys. Rev. **105** (1957) 288; See also the phase shift analysis by H. P. Stapp et al.: Phys. Rev. **105** (1957) 302.
9) T. Hamada and I. D. Jahnston: Nucl. Phys. **34** (1962) 382.
10) K. Nisimura: Prog. Theor. Phys. Suppl. **39** (1967) 286.
11) S. Otsuki et al.: Soryushiron Kenkyu **22** (1960) 20.
12) K. Nisimura et al.: Unpublished
13) N. Hoshizaki and W. Watari: Prog. Theor. Phys. **33** (1965) 337. P. Signell: Phys. Rev. **135** (1964) B1344.

H. P. Noyes et al.: Phys. Rev. **139** (1965) B380.
C. J. Batty and J. K. Perring: Phys. Letters **16** (1965) 301 See also Ref. 10.
14) K. Nisimura et al.: Institute for Nuclear Study, Univ. of Tokyo, INSJ-45 (1961).
15) P. Christmas et al.: Nucl. Phys. **41** (1963) 388.
C. J. Batty et al.: Nucl. Phys. **45** (1963) 481, **51** (1964) 225.
16) T. C. Griffith et al.: Phys. Rev. Letters **10** (1963) 444.
17) A. Ashmore et al.: Nucl. Phys. **65** (1965) 305, **73** (1965) 256.
18) J. Sanada et al.: Prog. Theor. Phys. **38** (1967) 1205, Nucl. Phys. **B4** (1968) 379.
19) N. Hoshizaki: Prog. Theor. Phys. **38** (1967) 1203.
20) R. M. Craig et al.: Nucl. Phys. **86** (1966) 113.
21) P. Catillon et al.: Nucl. Phys. **B2** (1967) 93.
22) See, for example, C. D. Jeffries: "Dynamical Nuclear Orientation," (John Wiley, New York, 1963).
23) T. Hasegawa et al.: Nucl. Instr. Meth. **73** (1967) 349.
24) J. Butterworth et al.: Proc. Phys. Soc. **91** (1967) 605.
25) N. Jarmie et al.: Phys. Rev. **155** (1967) 1438.
26) D. Garreta, K. Nisimura and M. Fruneau: Phys. Letters **31B** (1970) 363.
27) D. Garreta and M. Fruneau: Nucl. Phys. **A170** (1971) 492.
28) M. H. MacGregor et al.: Phys. Rev. **182** (1969) 1714.
29) R. Tamagaki and W. Watari: Prog. Theor. Phys. Suppl. **39** (1967) 23.
30) R. Tamagaki: private communication